Science Advances
AAAS

Supplementary Materials for

Compact holographic sound fields enable rapid one-step assembly of matter in 3D

Kai Melde *et al.*

Corresponding author: Kai Melde, kai.melde@mr.mpg.de; Peer Fischer, peer.fischer@mr.mpg.de

Sci. Adv. **9**, eadf6182 (2023)
DOI: 10.1126/sciadv.adf6182

The PDF file includes:

Other Supplementary Material for this manuscript includes the following:

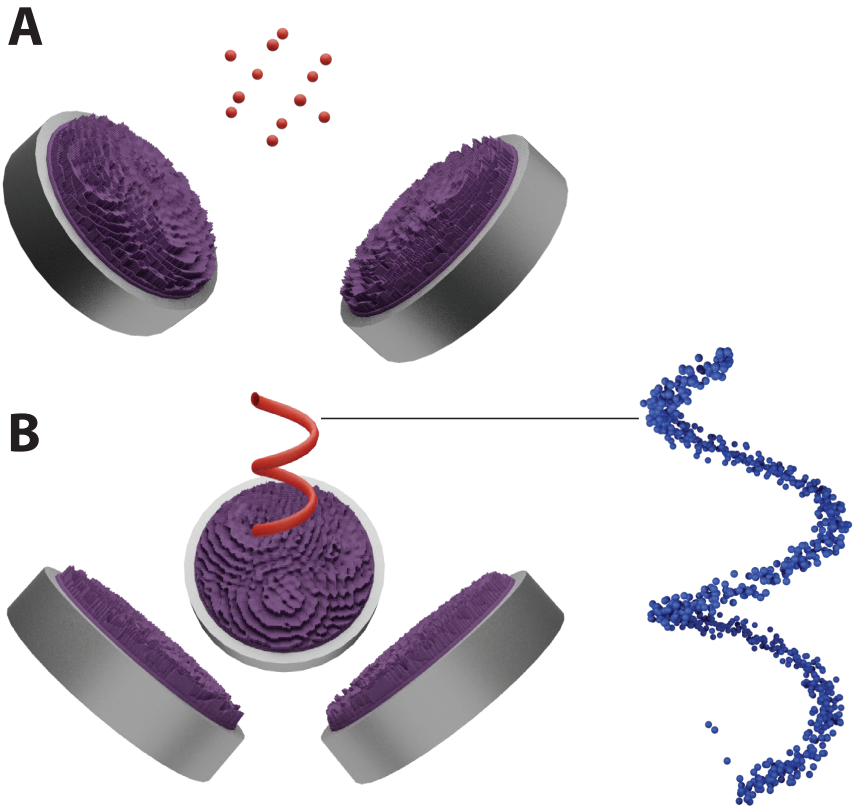

Figure S1: Configurations of transducers and holograms around the region of interest. Examples for (**A**) two and (**B**) three holograms.

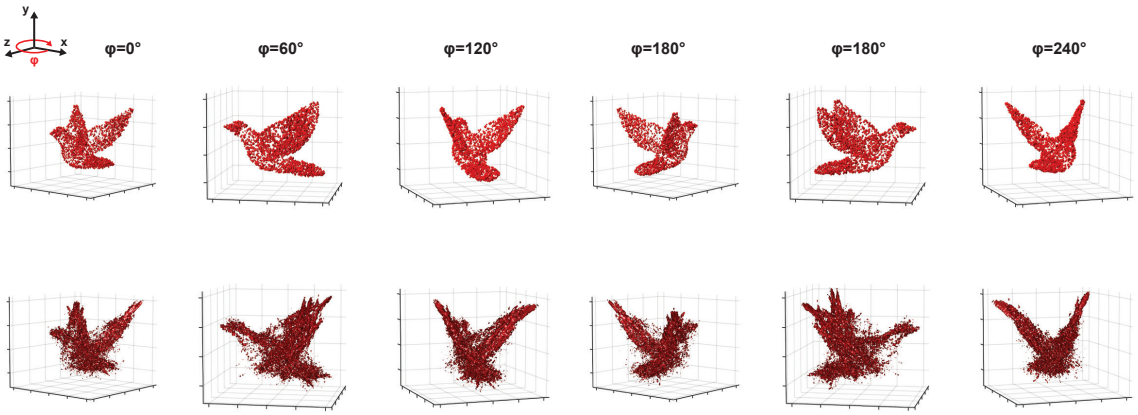

Figure S2: 3D image of a dove. Computed at 3.5 MHz, $\lambda = 420\,\mu$m. Rotated views of target image (top row) and simulation (bottom row). Grid spacing is 5 mm.

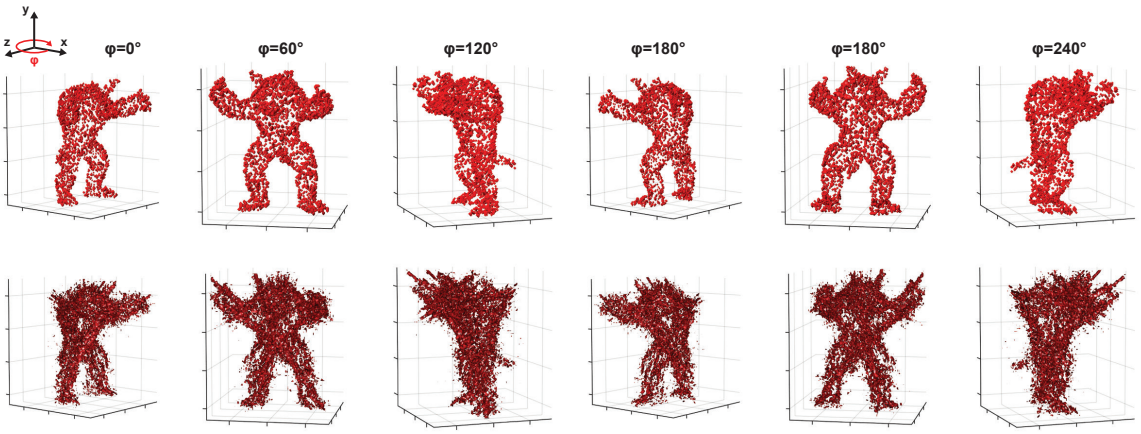

Figure S3: 3D image of the Stanford Armadillo. Computed at 3.5 MHz, $\lambda = 420\,\mu$m. Rotated views of target image (top row) and simulation (bottom row). Grid spacing is 5 mm. The model can be found at http://graphics.stanford.edu/data/3Dscanrep/.

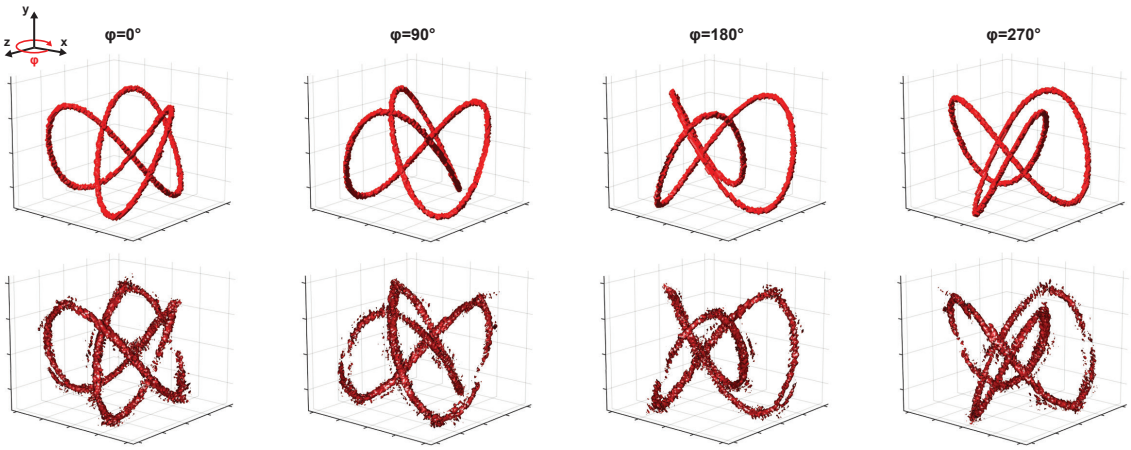

Figure S4: 3D image of a trefoil knot. Computed at 2.25 MHz, $\lambda = 660\,\mu$m. Rotated views of target image (top row) and simulation (bottom row). Grid spacing is 5 mm

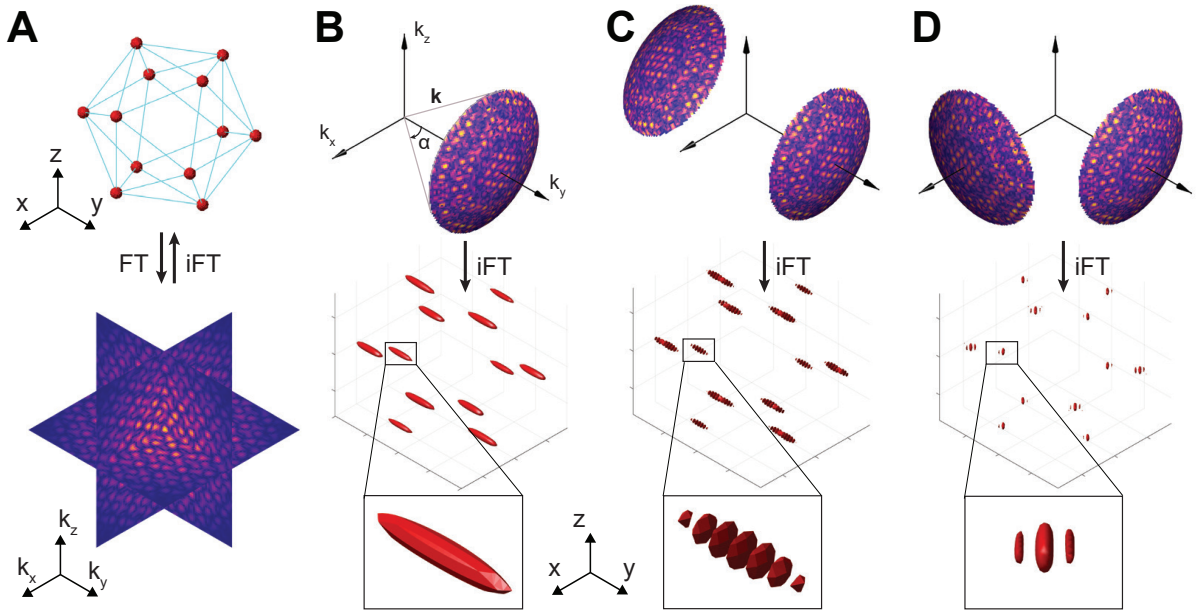

Figure S5: 3D Fourier spectrum and Ewald surfaces. (**A**) Focal points in the shape of an icosahedron and their 3D Fourier spectrum (bottom). The spectrum limited to (**B**) one finite source, (**C**) two opposing finite sources and (**D**) two orthogonal finite sources. The bottom row for panels (**B-C**) shows the corresponding field amplitudes and a magnified portion in an inset.

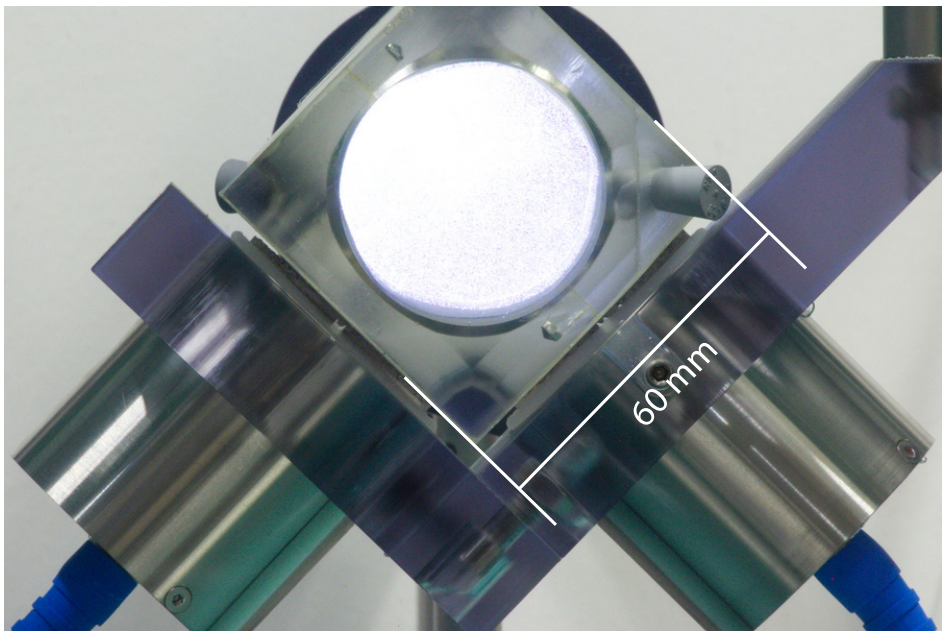

Figure S6: Photo of the experimental setup using two transducers. The rig is submerged under water. The air water interface is outside of the view towards the top.

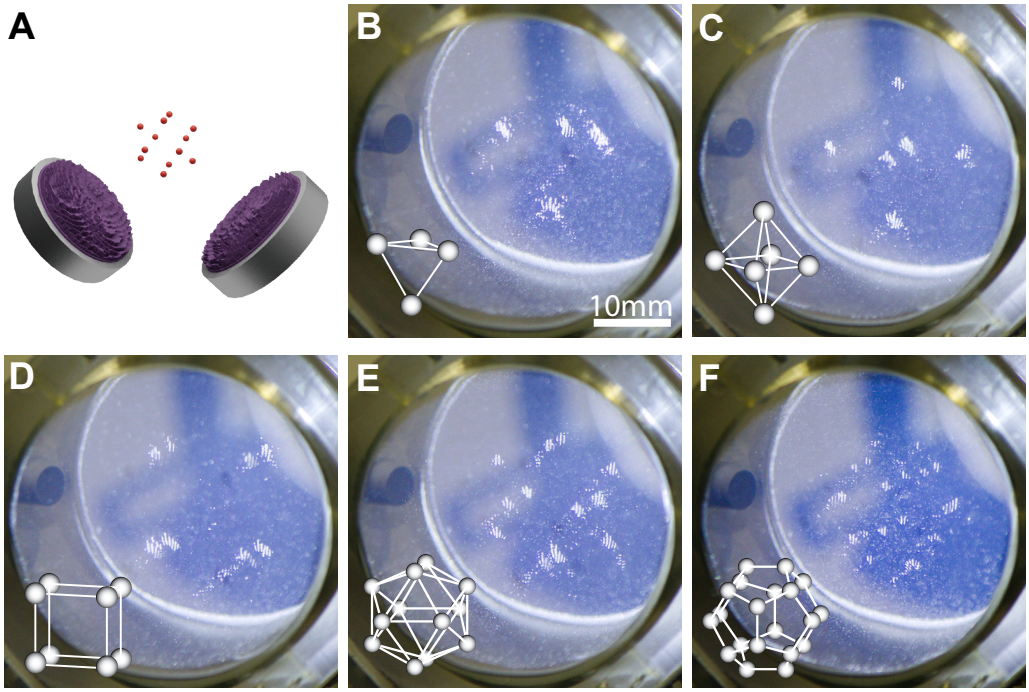

Figure S7: Trapping of silica microspheres at predefined points in 3D. (**A**) Schematic of the experimental setup using two holograms (sample container is hidden). The trap locations represent vertices of the platonic solids (scale bar 10mm): (**B**) tetrahedron, (**C**) octahedron, (**D**) cube, (**E**) icosahedron and (**F**) dodecahedron.

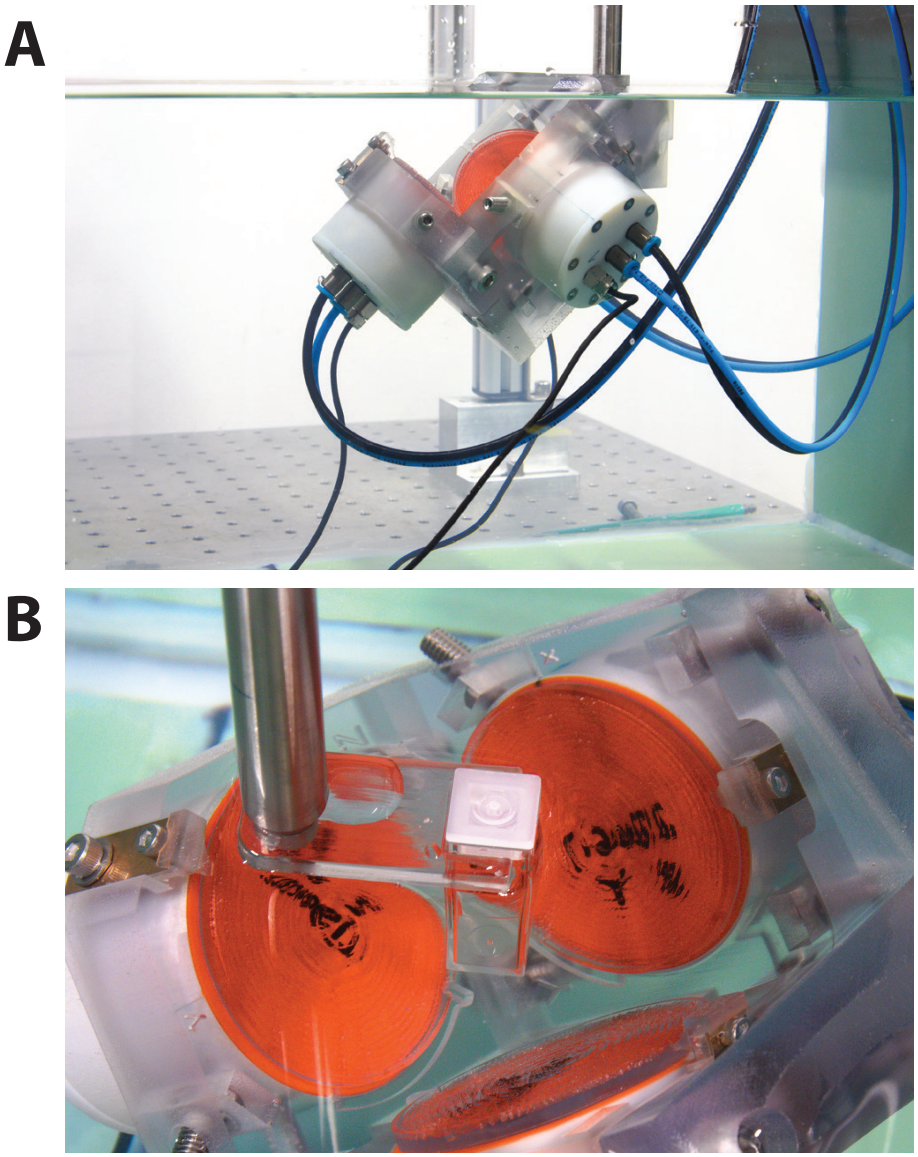

Figure S8: Photo of the experimental setup using three transducers. (**A**) side view. (**B**) top view with square UV-cuvette held in the region of interest.

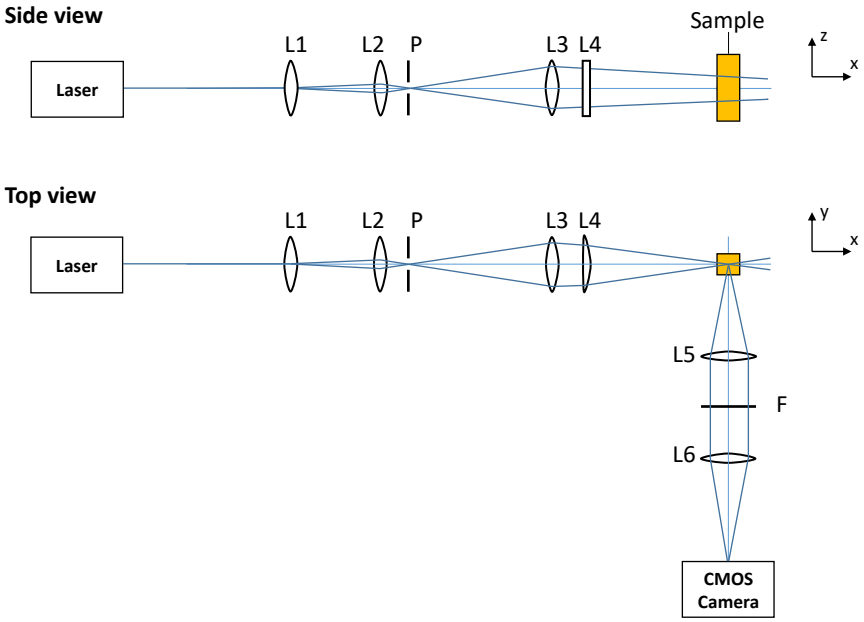

Figure S9: Laser lightsheet imaging. Schematic drawing of the setup.

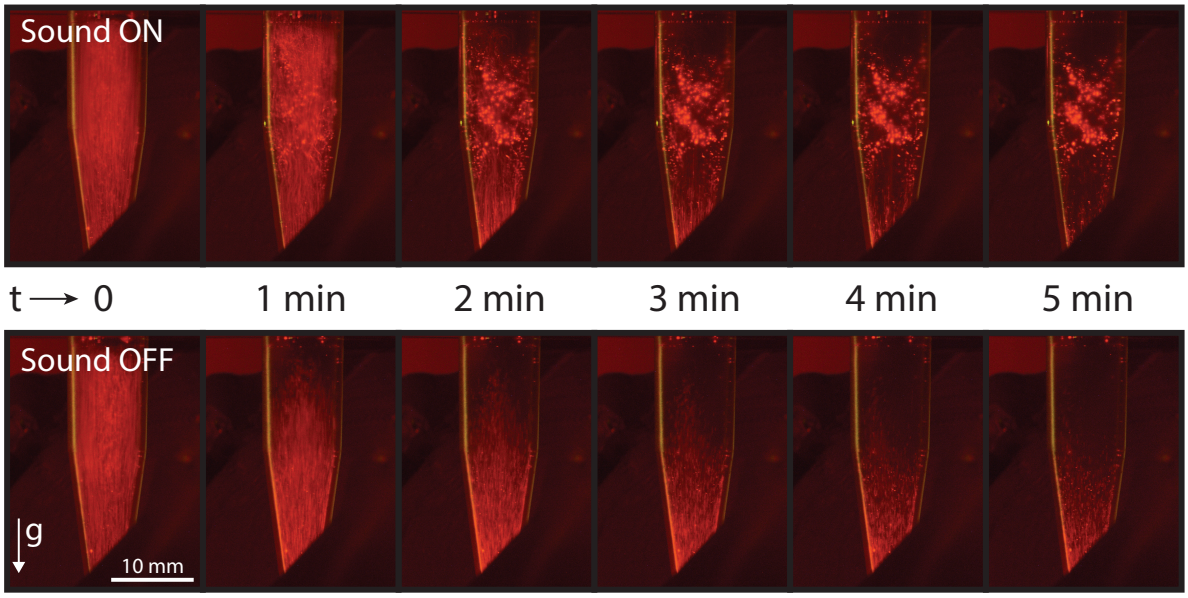

Figure S10: Sedimentation of hydrogel beads through an acoustic trapping field. The trap has the shape of an upright helix. Bottom row is the control experiment without sound, which confirms sedimentation of the beads to the bottom. Exposure time for each photo was 30 s

Movie S1 : **Assembly of an icosahedron.** This movie shows the trapping of silica gel particles at the vertices of an icosahedron. This has been accomplished using two transducers and holograms. The particle suspension is held inside a cubic container with thin circular windows. The cube is placed manually on the transducers and the ready sedimentation of the particles quickly reveals the location of the acoustic traps.

Movie S2 : **Assembly of a helix.** This movie shows the assembly of silica gel particles to a helix using three transducers and holograms. The particle suspension is held inside a cubic container with thin circular windows. The cube is placed manually on the transducers and the ready sedimentation of the particles quickly reveals the helix shape of the acoustic traps.

Movie S3 : **Animated views of the assemblies.** This movie shows animations of the 3D structures that were acquired using laser light sheet imaging as described in the methods section. Shown are a helix of silica gel particles, a figure 8 curve of hydrogel beads and a cluster of C2C12 mouse mybloast cells. The structures correspond to those shown in the manuscript in Figures 5 and 6.